A GIS-based Assessment of PHMSA Geohazard Bulletin Case Studies

Justin Oliveira[1], Sunil Chintalapati[2]
[1]Boston Geospatial, Inc., [2]Boston Geospatial, Inc.

Organized by

https://doi.org/10.52202/078572-0013

https://doi.org/10.52202/078572-0013

Abstract

Energy infrastructure is exposed to an active and ever-changing geohazard landscape, and regulators are raising the bar for operators to better quantify, prepare for, and mitigate potential impacts from these threats. On June 2, 2022, Pipeline and Hazardous Materials Safety Administration (PHMSA) released its updated advisory bulletin reminding owners and operators about the seriousness of geohazards. In this update they highlight various case studies involving failures due to or likely due to subsidence, landslides, seismicity, and more. Furthermore, the bulletin offers various suggestions for abatement including in-line inspection (ILI) surveys, in situ sensors, remote sensing, geotechnical surveying, and more. Because these hazards are so diverse, no one technology can adequately address them. Instead, a concert of solutions must be combined to ensure pipeline integrity and achieve the desired performance. This paper will explore case studies referenced in the bulletin using a GIS-based geohazard tool funded in part under the PHMSA Pipeline Safety Research and Development Program. The paper will combine terrestrial, airborne, and satellite measurement phenomenologies to explore the case studies and demonstrate the tools use for identifying and measuring geohazard risk and estimating the anticipated mechanical loading.

Introduction

Geohazards

Geohazards refer to natural geological processes that pose risk to humans, property, and the environment. These events can include earthquakes and faulting, eruptions, landslides, sinkholes, ground subsidence and other terrain instabilities, all of which are driven by natural Earth processes (see **Figure 1**). Geohazards can have devastating impacts on communities, sometimes resulting in the loss of life but almost always resulting in property damage and subsequent economic loss. Geohazards, while primarily geological in nature, can also be triggered or exacerbated by changing climate patterns and events like excessive rainfall, freeze-thaw cycles, and more.

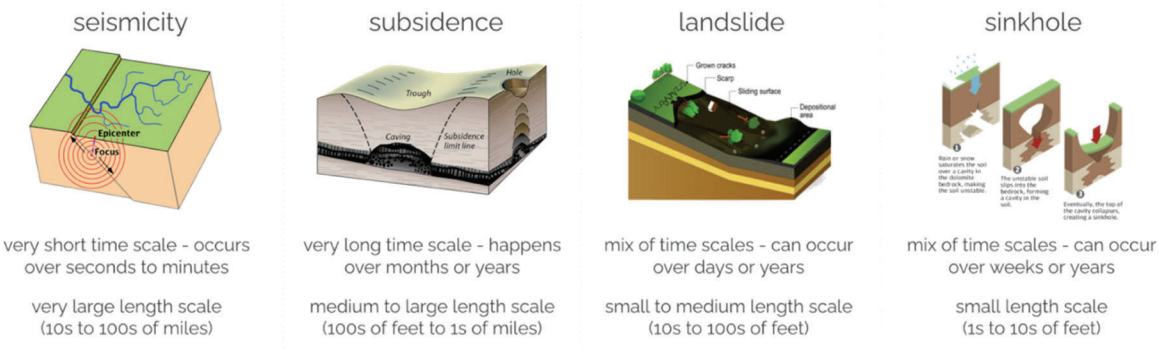

Figure 1. Summary view of time- and length-scales for various geohazards

Over the past decade, the United States has seen a noticeable shift in its geohazard landscape, particularly with an increase in landslides and sinkholes. Factors such as extreme weather events, driven by changing climate patterns, have led to more landslides, especially in regions prone to heavy rainfall and seismic activity. Meanwhile, sinkholes have become more common in areas with soluble

https://doi.org/10.52202/078572-0013

rock substrates, such as Florida, exacerbated by groundwater extraction and land development, highlighting the growing impact of human activities on geohazard dynamics.

Geohazards can severely impact buried pipelines by subjecting them to excessive stress and strain, thereby creating challenges for integrity management. Geohazards can induce abnormal loads and deformations, which pipelines may not have been designed to withstand. For example, landslides can exert powerful lateral pressures, causing pipelines to bend beyond their design limits. Seismic events can produce ground shaking and fault displacement, inducing axial and bending strains as well as shear stress in pipelines that may lead to buckling or ruptures. Sinkholes can cause a sudden loss of support, resulting in sagging and increased dead loading. These stresses and strains can compromise the pipeline, leading to leaks or bursts that necessitate immediate and costly repairs and pose significant environmental and safety risks. Understanding which sections of a pipeline may be exposed to these geohazards and quantifying their exposure is crucial.

Incident Statistics

In the PHMSA lexicon, geohazards are a type of Natural Force Damage. Geohazards include such threats as seismicity and faulting, earth movement, landslides, and sinkholes. As it relates to buried piping, geohazards often manifest as longitudinal loads (e.g. axial forces from landslides, seismicity and faulting) or bending moments (e.g. sinkholes - unsupported dead/live loads, perpendicular landslides, and earth movement).

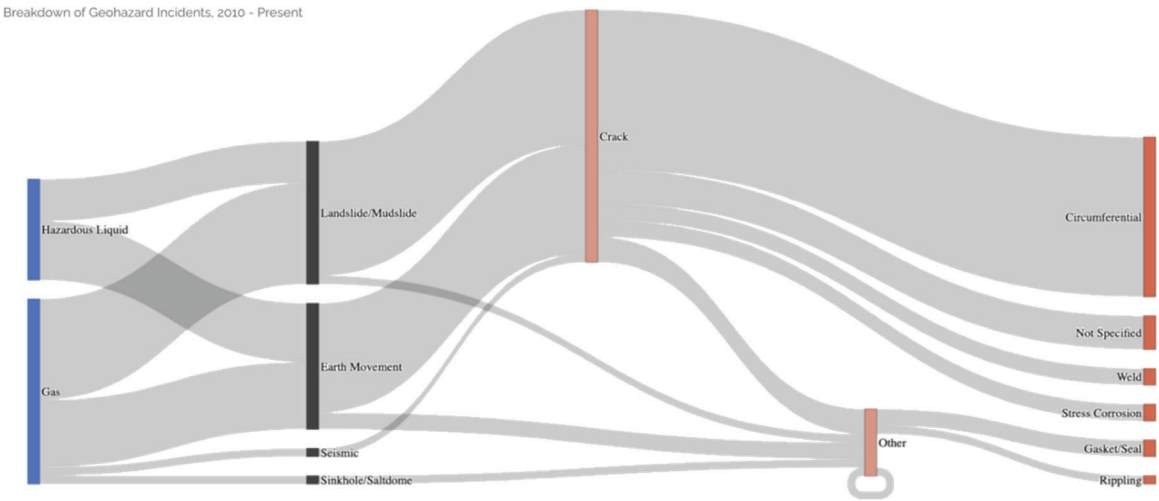

Figure 2. Summary of geohazard incidents, proximate and root causes

Regardless of whether the pipeline is part of a gas or hazardous liquid system, most incidents over the past 13 or so years stemming from geohazards have been due to landslides and earth movement [1]. Given that many geohazards render themselves as longitudinal loads, most failures come from circumferential cracking (see **Figure 2**). While every system is unique to a certain degree, some generalizations can be extracted from the incident data. On average, landslides are oftentimes more catastrophic than earth movement incidents, because of that there is usually more damage to the system. The direct cost of a geohazard-related failure varies but is in the range of $4-6mm for landslides and $1.5-3mm for earth movement. Ignitions and explosions are very rare in hazardous liquid geohazard incidents, whereas in gas systems it occurs in roughly 1 out of every 5 incidents.

https://doi.org/10.52202/078572-0013

PHMSA Guidance

PHMSA has issued two notices on geohazards - the first in 2019 [2] and an update in 2022 [3]. These notices emphasized a couple key things to operators: (i) the role of patrolling programs in identifying slowly developing or acute geohazard events; and (ii) the tie-in to existing Code of Federal Regulations (CFR) language holding them responsible for identifying and managing these threats relative to their integrity management efforts. Within these bulletins, PHMSA provided several geohazard incident case studies involving buried gas and hazardous liquid pipelines. Furthermore, PHMSA provided numerous recommendations to operators, which include (but are not limited to) geohazard screening of areas around pipelines; develop monitoring plans based on site-specific risks; and utilize remote sensing technologies to measure changes in ground conditions.

CFR and Standards

Buried pipelines experience various types of loads which must be considered in the design and evaluation of the system. A complete mapping of load type from the CFR [4, 5], down through to the applicable American Society of Mechanical Engineers (ASME) codes [6, 7], and then into other guidelines or literature references were performed by the authors. Part 192 and 195 either directly or indirectly reference requirements for various load types. Some of these types are mentioned by name in the CFR, such as pressure and thermal loads, and a design equation and other guidance is provided. The loads not mentioned by name in the CFR are still required to be included in the design and evaluation of a system because of the reference to ASME B31.8 or B31.4. Furthermore, while B31.8 and B31.4 mention geohazard loads (as well as other non-geohazard loads such as live and dead loads), they do not themselves have design equations and guidance on load development. In place of these gaps, industry guidelines as well as literature sources and subject matter expert (SME) input were used - an example is shown in **Table 1** below.

Table 1. Sample load development with CFR flow down

Load Type	CFR	Code	Source Equation
Seismic	192.103	ASME B31.8 - 841.13a	ASCE (2001) Guideline for the Design of Buried Steel Pipe [8]
	195.110	ASME B31.4 - 403.6.2.6	

Each of the load types considered by the tool are classified as either sustained or occasional loads (see **Table 2**).

Table 2. Load type classification for combined stress modeling

Load Treatment for Combined Stress Estimation	
sustained load	***occasional load***
internal pressure, thermal (expansion and contraction), dead and live surface loading, earth movement, sinkhole	landslide, seismic, faulting

This classification is then later important in determining the combined stress, allowable stress, and stress margin in accordance with the applicable design code.

https://doi.org/10.52202/078572-0013

Tool Architecture

To assess geohazard exposure and potential impacts to pipelines over large areas, a geospatial tool was developed by the authors (see **Figure 3**). The tool leverages the operators pipeline data model implemented in ArcGIS and combines it with both first- and third-party geohazard data to evaluate potential exposure, performs dynamic segmentation of the pipeline to develop load cases, and then formulates and applies boundary conditions to design equations to ultimately evaluate the mechanical stress conditions. The tool can also be used outside of ArcGIS and integrated with other pipeline integrity management and damage prevention platforms.

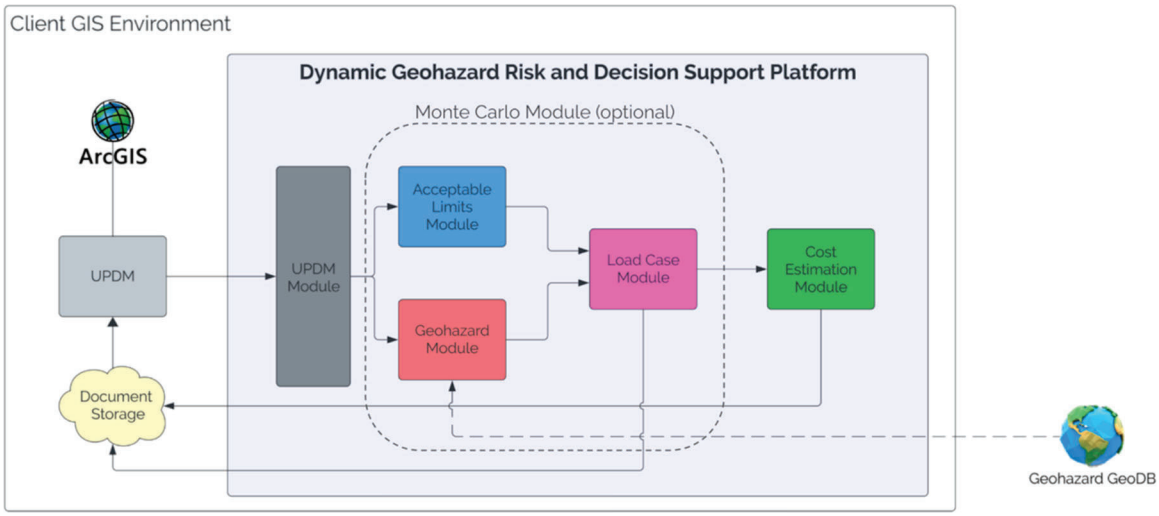

Figure 3. Diagram of the geospatial geohazard tool

Piping information and other relevant parameters are extracted from the end-user's pipeline data model, which supports Esri Utility and Pipeline Data Model (UPDM) [9] directly. For Pipeline Open Data Standard (PODS) [10] models, support has been added temporarily to map model data into the UPDM framework until full support for PODS is integrated into the tool. The segmentation done by the tool is stored as a feature layer within the model project file. Furthermore, imported datasets are stored as feature layers in the model along with the intermediate and final calculations, preserving the relational mapping back to the pipeline data model.

A series of modules exist to import and prepare data needed to perform the geohazard surveys and modeling. Currently these imported datasets include the authors' geohazard data stored in a cloud-based geodatabase, however they can be tailored for other first- and third-party datasets - e.g. Light Detection and Ranging (LiDAR), etc. Additionally, soil data is imported such that pipe-soil interactions can be modeled in the loading - currently the tool leverages an enhanced version of the United States Department of Agriculture (USDA) Soil Survey Geographic Database (SSURGO) developed in-house by the authors but can also utilize end-user data as well. Lastly, vector data from OpenStreetMap (OSM) [11] detailing natural and manmade surface features are imported and augmented to help drive pipeline segmentation and load case development. Beyond their use for segmentation of the pipeline and creation of the load cases, these datasets are also used to develop the boundary conditions in the design equations from which stresses are evaluated.

https://doi.org/10.52202/078572-0013

To successfully investigate the impact geohazards may have on a piping system, an appropriate set of load cases must be developed. These load cases will vary spatially along the system depending on localized exposure to geohazards, system configuration, and other factors. Spatial analysis is used to perform the segmentation of the piping network. Following this, the pipeline is further segmented into subsections such that no segmented section is larger than a set span which can be controlled by the end-user (but recommended to be no larger than 1,000 feet). This maximum span control allows for the proper evaluation of seismic loading over sections exposed to no other loads except nominal loads (pressure, temperature, and dead load).

Segmentation is performed on the pipeline layer as follows: The process begins with an intersect analysis to identify pipeline segments affected by each non-geohazard layer (e.g., roads, railways, runways, waterways) and geohazard layers. Geohazard layers may include karst and sinkholes, fault lines, earth movement detected via differential LiDAR or interferometric synthetic aperture radar (InSAR). Once the intersect layers for each non-geohazard and geohazard layer are generated, they are added as feature layers in the pipeline data model.

The next step involves retrieving the pipeline layer along with all intersect layers as geodataframes, with the coordinate reference system (CRS) set to World Geodetic System 1984 (WGS84). The pipeline layer, now in WGS84 CRS, is used as the input layer for intersection checks with the first intersect layer. This operation produces an output file containing the pipeline segmented based on the first intersect layer. Subsequent intersect layers are applied iteratively, further segmenting the pipeline layer progressively. The final segmented pipeline includes columns indicating whether each segment intersects with a specific layer (1 for intersection, 0 for no intersection). Note that a single pipeline segment may intersect with multiple non-geohazard and geohazard layers, a single layer, or none at all. This fully segmented layer is then stored as a feature layer within the pipeline data model. Each segmented section of the pipeline has its own load case table for which boundary conditions are developed and stress and margin calculations are performed - this data is stored in companion tables within the ArcGIS project.

Design equations following the CFR and subsequent ASME code as well as modeling approaches from an extensive literature review are then used with the pipeline attributes and load case information to model all the applicable loads - this included pressure, temperature, live and dead loading, and of course geohazards. Once the loads are estimated, the stresses are collected and combined in accordance with ASME B31.8 (gas) and B31.4 (hazardous liquid). Buckling checks are carried out for each section of the pipeline and then the margins are evaluated.

All calculation steps along the workflow are performed for the nominal values of all determinants, however Monte Carlo simulations can also be used as well if there is uncertainty about or quantified variability of model parameters (e.g. depth of cover, wall thickness, landslide runout distance or direction, soil moisture, etc.) The intermediate calculations and combined stress and margin calculations (including indication of driving stress and margin sources) are all stored in companion tables in the ArcGIS project. The data can then be visualized using a set of pre-canned or custom table, graph or map views.

https://doi.org/10.52202/078572-0013

Geohazard Modeling

An exposure and susceptibility assessment is done to the pipe system using several curated datasets. These datasets help spatial segment the system into affected sections as well as derive the appropriate boundary conditions for stress modeling. What follows is a summary of the geohazards included in the tool, how each type is modeled in terms of mechanical loading, and the sources and methods for deriving the dependent variables necessary to evaluate the load cases.

Seismic

Seismic events create transient strains in the pipe due to ground shaking and wave propagation. Here only longitudinal (axial) strain is considered since bending (flexure) is considered negligible given the pipe diameter relative to ground-surface curvature. The wave propagation causes compression and expansion of the soil along the longitudinal direction, but the axial strain imparted onto the pipe is limited by the friction at the pipe-soil interface (see **Figure 4**).

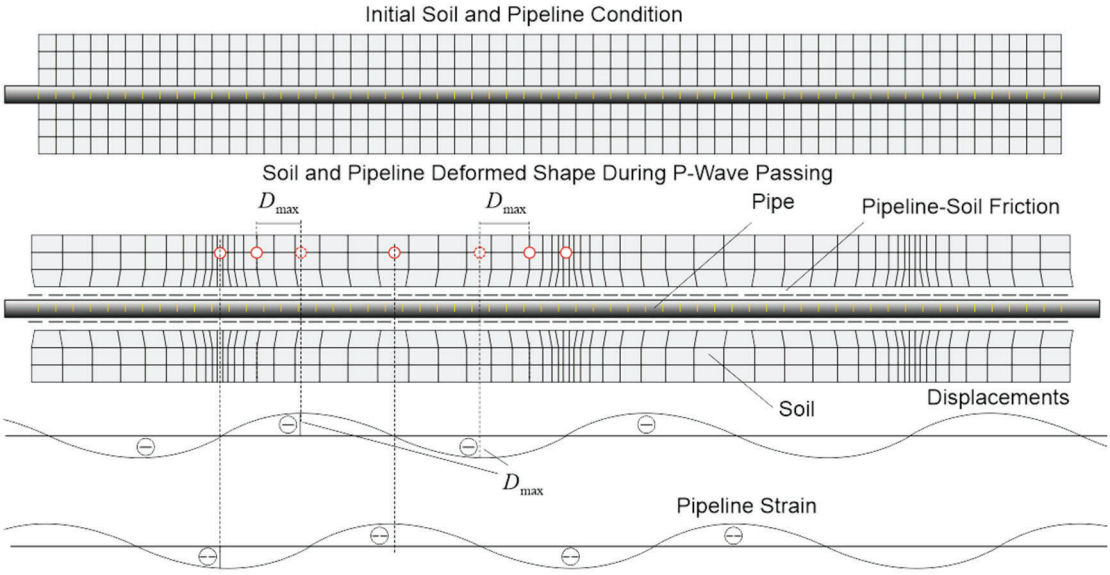

Figure 4. Plot of soil movements from seismic wave [12]

The stress resulting from an episodic seismic event is found by estimating the axial strain along the pipe section using seismograph data [13] and/or American Society of Civil Engineers (ASCE) 7 standard [14], namely the peak ground velocity (PGV), with seismic modeling as well as soil models (namely axial soil friction force) and the pipeline data model. The PGV is estimated for the pipe section based on the event attributes and then from this the axial strain is calculated directly [15, 16, 17, 18]. The strain is then translated into a stress using dimensions and properties from the pipe data model.

Faulting

Seismic events are accompanied by permanent fault movement which can oftentimes propagate to the surface near where pipelines are buried. These deformations can occur regardless of whether the seismic event was of high intensity and induce an axial strain in the crossing pipeline(s). There are different types of fault motions (e.g. strike-slip, reverse fault, etc.), some of which are shown in **Figure**

https://doi.org/10.52202/078572-0013

5 below, but generally the result is a relative displacement of the ground horizontally and/or vertically that permanently (plastically) deforms the pipe.

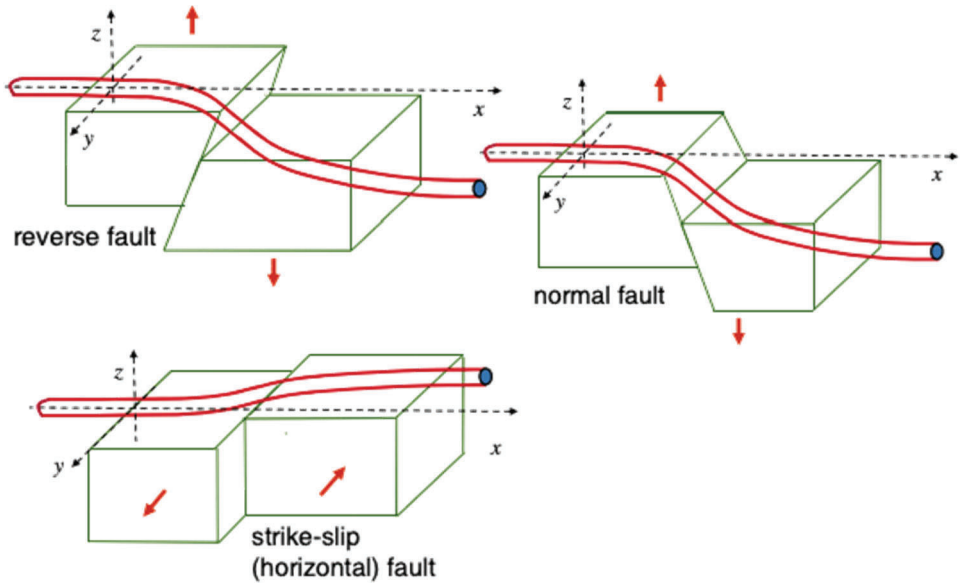

Figure 5. Pipeline crossing various fault configurations [19]

Fault motion during seismic events can create significant stress on buried pipelines, leading to potential damage or failure. When a fault activates, it can cause the ground on either side of the fault line to move in opposite directions. This differential ground movement can directly impart stress on buried pipes, especially if they cross the fault perpendicularly or at an angle.

The axial stress resulting from a slow or rapidly slipping fault is found by estimating the axial strain along the pipe section using sensed fault kinematics (ground displacement), fault geometry models, and the pipeline data model attributes [20]. The axial strain from faulting is generally limited by the peak friction force of the surrounding soil. A geodatabase with mapped fault line data from the Global Earthquake Model (GEM) Foundation's Global Active Faults dataset [21] and United States Geological Survey (USGS) National Seismic Hazard Models (NSHMs) dataset [22] is used but other datasets can be ingested as well. If the pipe section crosses an active fault, the kinematics are found and used in a forecaster to estimate peak ground displacement (PGD) over a time horizon (e.g. time between ILI runs) - alternatively, the forecasting can be skipped, and net fault movement be prescribed instead. Once this fault motion is found, these movements are transformed into the pipe coordinate frame and the axial strain is estimated directly, and stress is estimated using the pipe data model.

Earth Movement

Earth movement, either from subsidence or other processes, is a significant geotechnical concern that can have profound impacts on the integrity and functionality of buried pipelines. Subsidence, the gradual settling or sinking of the earth's surface, can occur due to natural processes or human activity (mining or excessive groundwater extraction). When the ground moves in this way, it can impose bending loads on buried pipelines. These loads can compromise the structural integrity of the pipelines, increase maintenance costs, and pose significant risks of leaks or catastrophic failures,

https://doi.org/10.52202/078572-0013

potentially leading to environmental contamination and safety hazards. Therefore, understanding and mitigating the impacts of earth movement is crucial in the design, maintenance, and monitoring of buried pipeline infrastructure.

To measure earth movement conditions around infrastructure, space-based InSAR is utilized. InSAR is a cutting-edge remote sensing technology that utilizes radar signals from satellites to measure the changes in terrain with high accuracy over time. By comparing radar images acquired at different times, InSAR can detect and measure the small differences in the phase of the radar signals, which correspond to ground movement between the satellite passes - from this ground kinematics around infrastructure can be extracted (see **Figure 6**). While InSAR is an impressive technology, it is limited in its ability to discern motion orthogonal from its look direction (typically motion in the North-South or South-North direction). For this reason, the tool only utilizes InSAR for non-landslide related ground motion - this could include pre-collapse motion related to sinkhole emergence, subsidence from aquifer or well depletion, uplift from injection operations, freeze-thaw in permafrost or non-permafrost regions, etc.

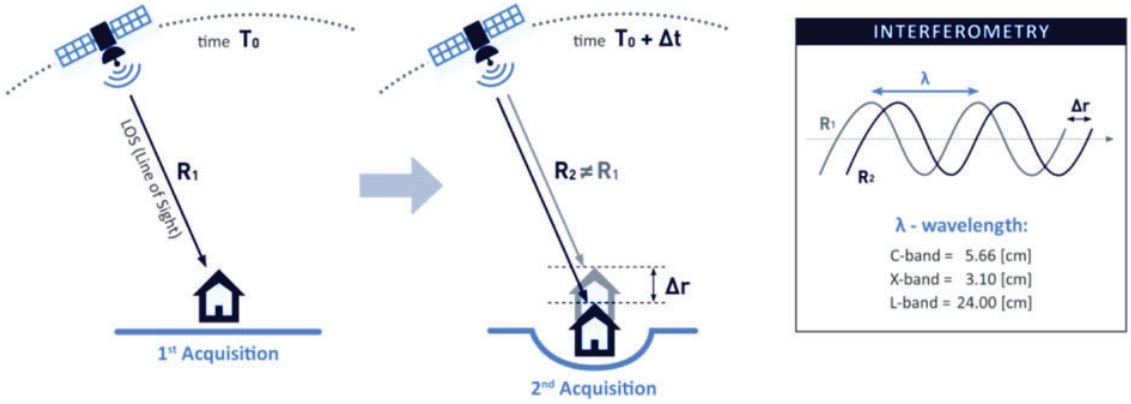

Figure 6. Two-pass measurement showing change in phase associated with ground displacement [23]

The longitudinal bending moment resulting from earth movement is found by estimating the bending strain along the pipe section using remotely sensed ground kinematics (geodetic motion decomposition and transformed into the pipe reference frame), soil models (lateral and vertical soil stiffness and bearing capacities), and the pipeline data model (coupled pipe-soil stiffness). If the tool determines a pipe section crosses an area with observed ground motion (done by performing a spatial crossing analysis with a geodatabase of InSAR data), the kinematics are found and used in a forecaster to estimate the ground displacement over a time horizon (e.g. time between ILI runs).

Earth movement causes changes in the pipeline curvature, which results in bending strain and stress in the longitudinal direction (see **Figure 7**). This load is resisted by the soil compliance, which depends on the backfill material in the pipe trench and other factors.

https://doi.org/10.52202/078572-0013

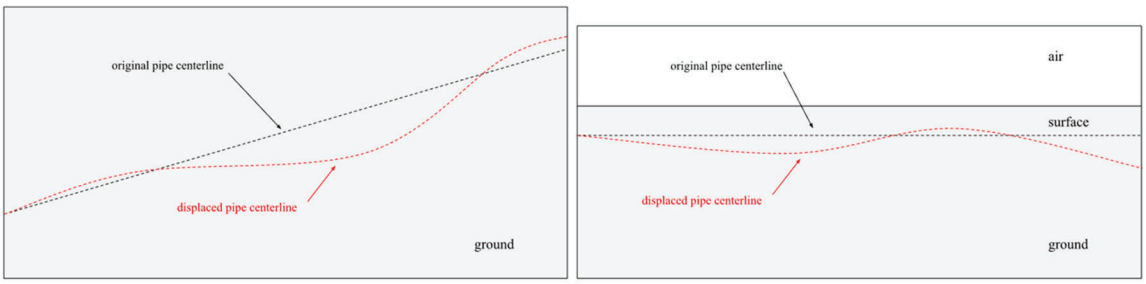

Figure 7. Pipe centerline under earth movement with resulting change in position and line curvature, causing bending strain/stress

The observed ground motion from InSAR is combined with a coupled pipe-soil spring system to estimate the ground movement at the pipe-soil interface - this is then used as a boundary condition to calculate the stress and strain from earth movement along the impact areas of the pipeline.

Landslide

When a landslide occurs, massive soil movement can displace the ground in which pipes are buried. This can lead to axial force-related stress, where the pipe is subjected to compressive or tensile forces along its length, potentially causing it to shorten or elongate. Moreover, the differential movement of soil can induce bending strain, where the pipe bends under the uneven pressure, leading to potential deformation or rupture. The severity of the impact on buried pipes during a landslide depends on factors such as the depth of cover, the pipe material and design, the landslide orientation and displacement relative to the pipe.

Landslide formation and processes are a complex topic, and there are tools to model these dynamics (e.g. Stantec DebrisFlow Predictor, GEO5, etc.) However, the tool herein requires a much simpler model that can be run at scale over large networks to provide an initial loading scenario for stress-strain assessments. To accomplish this, the authors first identify landslide prone areas through landslide susceptibility modeling and then model runout separately assuming failure.

To assess the susceptibility of the terrain to landslides, an infinite slope model is developed of the pipeline right-of-way and adjacent areas - from this, the conditions can be modeled and propensity for slippage evaluated using Coulomb's law. The ratio of static force balances (resisting forces to driving forces) in the slope, factor of safety (FS), is assessed using a LiDAR-based digital elevation model (DEM) model, soil mechanical properties, and soil saturation data. A FS less than 1 means the slope is susceptible to failure. From the authors' own extensive back-testing against the USGS landslide inventory and other published research [24], a FS less than or equal to 1.2 is generally considered highly susceptible to landslide. For a given scene, once the slope model is complete using five or more years of historical soil moisture data, a landslide susceptible inventory is constructed and automatically written to a geodatabase for pipeline crossing and other analyses.

Once a slope or portion of a slope is inventoried, runout is estimated to develop boundary conditions for stress modeling. To accomplish this, a combination of geographic analysis with empirical modeling is employed (see **Figure 8**). Once slope areas along the pipeline are identified as susceptible to landslides, their locations along with terrain data (elevation data and soil properties) are extracted. The susceptible area is discretized into a cluster of points along the slope for which the gradient direction is evaluated - along this gradient, emanating from each point, a ray is constructed traveling

https://doi.org/10.52202/078572-0013

down the slope. The difference in height between the starting point and the toe is calculated - the toe is approximated by finding the location along the ray in which the slope angle is equal to half the friction factor. An empirical model [25] relating the height difference to the runout length is then used.

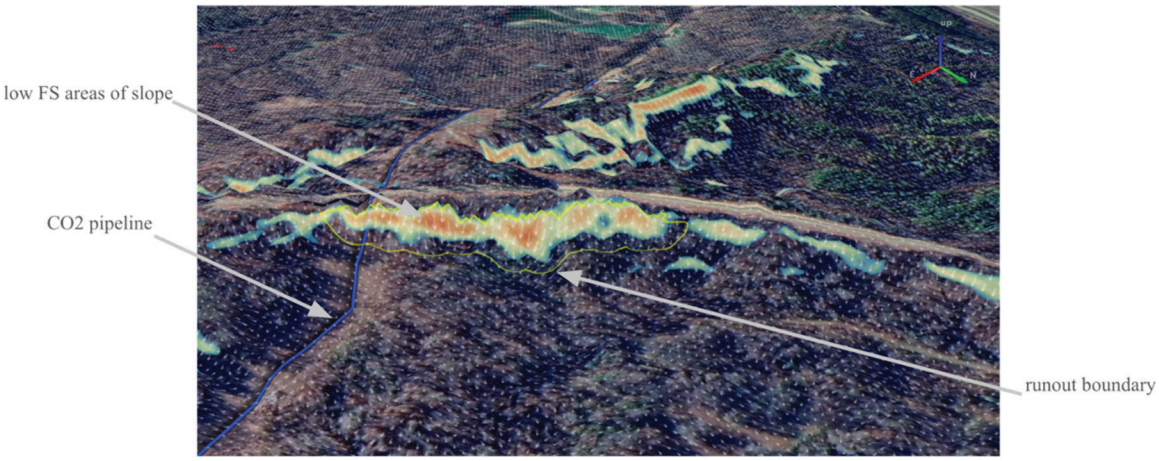

Figure 8. Example of failed slope along CO2 pipeline showing low FS areas and estimated runout boundary of landslide

To get the necessary boundary conditions for use in the pipe stress calculations, interpolation is done to map the runout direction and distance from the points within the susceptible region to the pipe. The orientation of the pipe in the geodetic frame known, the peak ground displacement and angles relative to the pipe coordinate frame are then determined.

Sinkhole

Sinkholes pose a significant risk to buried pipes by creating voids in the ground that can lead to uneven support and concentrated stress points. When a sinkhole forms near or beneath a buried pipeline, part of the pipe may lose its supporting ground, causing it to sag or bend due to gravity and the weight of the material it carries (i.e. dead and/or live loading). This results in bending moments on the impacted pipe sections. These moments are maximal where the curvature is greatest, typically at the points of support just outside the void. Over time, the stress from these bending moments can lead to fatigue, cracks, or even rupture of the pipe, especially if the material is brittle or has been weakened by corrosion or other factors.

Given the lack of a priori knowledge of where sinkholes are located around a piping network, a proxy must be used to gauge susceptibility. To accomplish this, the USGS formation maps [26] are utilized to filter out regions with rock types not typically associated with karst and/or sinkhole formation - typically karsts and/or sinkholes form in limestone, sandstone, and sandy-like formations. What remains is a map of areas where sinkholes are more likely to occur, which is used in a crossing analysis with the pipe network. If a section of the pipe network crosses one of these areas, it's assumed that any segment along that affected section could be exposed to an additional bending moment from a sinkhole (see **Figure 9**).

https://doi.org/10.52202/078572-0013

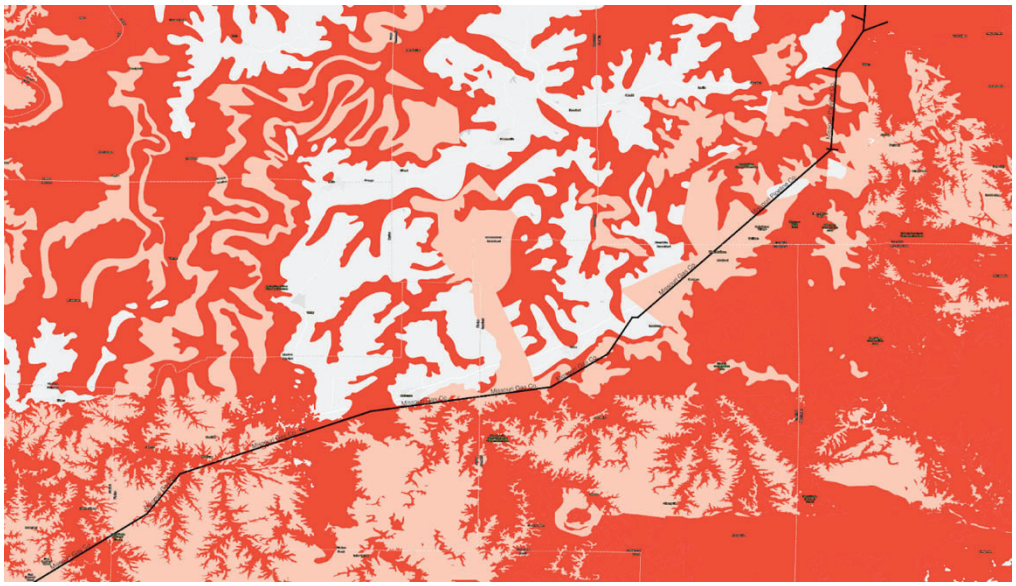

Figure 9. Sample area showing karst-prone regions (red) with pipeline; red shades proportional to average sinkhole size

The boundary condition for the moment calculation is the unsupported length for which dead and live loading is applicable. To provide an estimate for the unsupported length, a dataset was compiled on reported sinkholes (example references [27, 28]) and cross referenced it to the primary and secondary rock types from the USGS maps to arrive at summary statistics (i.e. average sinkhole diameter, depth, etc.) based on the underlying formation types. A lookup table is then used relating the primary rock type for the affected pipe segment to the average sinkhole dimensions.

Figure 10 shows applicable dimensions and a diagram of a worst-case situation of a pipeline with a Karst cavity formed underneath resulting in an unsupported length. A continuous uniform load is assumed across the supported and unsupported lengths from the dead load and the concentrated live load.

https://doi.org/10.52202/078572-0013

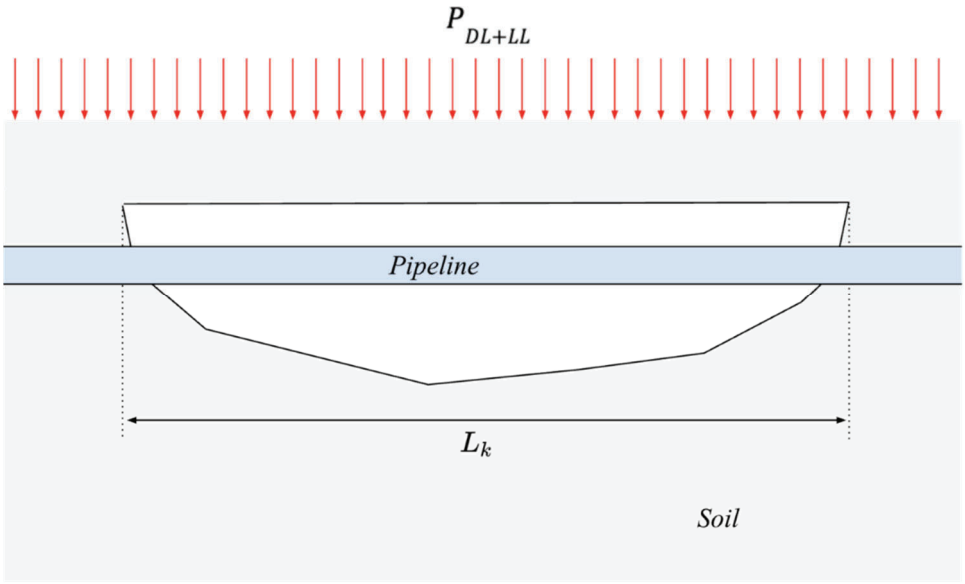

Figure 10. Diagram of karst with dead (P_{DL}) and/or live loading (P_{LL})

The longitudinal stress resulting from a sinkhole forming below a section of pipe is found by estimating the bending moment resulting from an unsupported dead and live load. The previously estimated dead and live load is used to directly estimate a worst-case bending moment - the bending moment is then translated into a longitudinal stress.

Case Studies

Using the methodologies and workflows discussed above, the tool can be used to perform risk assessments and support monitoring as well as aid forensic analysis. As part of the tool's verification and validation (V&V) effort, postmortem assessments of prior geohazard-related incidents were utilized. To perform these analyses, the authors relied on pipeline information only available in the public domain from PHMSA incident logs [29]. However, these incident logs don't include all the required information about the pipeline and conditions, so parametric variation of unknown parameter guided by subject-matter expert input was utilized.

Case Study 1: 2012, Virginia Natural Gas

In 2012, a gas leak was discovered in a Class 2 section of a 24" transmission line owned by Virginia Natural Gas. The section was exhumed and sent out for lab testing, which indicated that either a single severe bending moment or several less catastrophic bending moments caused the failure. The subsequent conclusion was that bending moments likely resulting from a recent earthquake compromised the weld-end insulator nearby a station resulting in cracked epoxy at the gasket. The seismic event in question was a M5.8 earthquake approximately 40 miles northwest of Richmond, Virginia which occurred in August of 2011 [30]. The earthquake most notably damaged the Washington Monument and National Cathedral in D.C. and caused $200-$300mm in damage [31].

As previously mentioned, unless limited by the soil load capacity, the maximum axial strain within a pipe during a seismic event is proportional to the PGV. At the location of the gas leak, the ASCE 7

https://doi.org/10.52202/078572-0013

design load equated to a PGV of 3.7 cm/s however the actual event was nearly double that at 7.8 cm/s. All the available seismic data from the USGS archive over the past hundred years was processed into PGV estimates. The ASCE 7 and actual incident were 4.6 σ and 10.6 σ events respectively (see **Figure 11**).

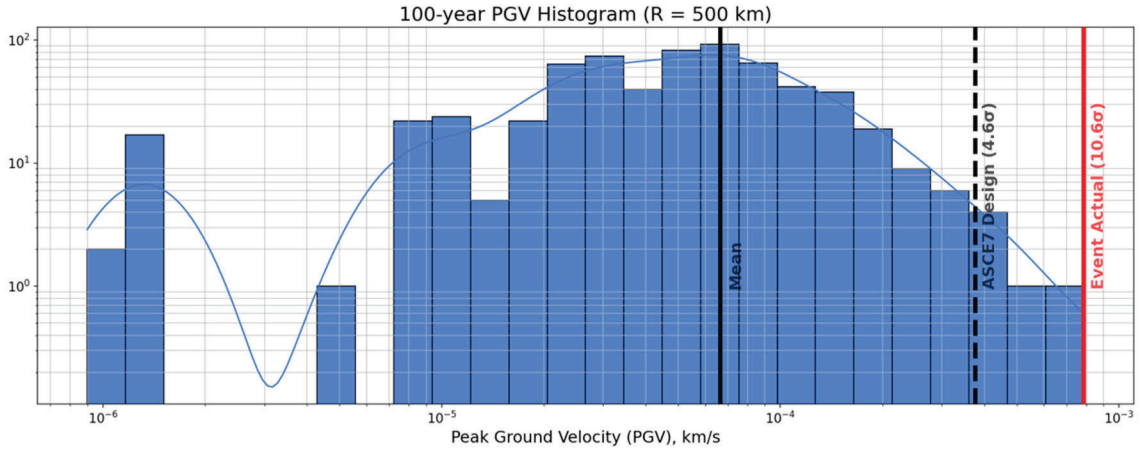

Figure 11. Histogram of estimated PGV values from historical seismic events

Information about the pipeline was limited in the PHMSA incident log, however some reasonable assumptions about its design for missing parameters was made, namely that (i) the material was American Petroleum Institute (API) 5L steel pipe; (ii) its wall thickness was between 0.375" - 0.75"; and (iii) the specified minimum yield strength (SMYS) was between 50 - 65 ksi. The basis for the wall thickness range came from standard, off-the-shelf vendor catalogues based on its listed maximum allowable operating pressure (MAOP) as well as ranges from similar pipelines. The strength range came from 192.105 and ASME B31.8 flow down – other material properties were found from their respective specification and acceptable ranges. Other model parameters were unknown and thus varied over all possibilities – for example bedding design and surface finish (varied across all options), temperature conditions varied based on historical National Oceanic and Atmospheric Administration (NOAA) data, etc.

The tool estimates other information about the pipeline required for loads development and margin assessment – for example the sections proximity to nearby road for live loading as well as soil properties required for evaluation of dead, live, and geohazard loads. The tool was then used to evaluate potential exposure to geohazards – for the affected section a seismic and sinkhole load case was found. The hoop (dead load, live load, and operating pressure) and longitudinal loads (operating pressure, thermal, and seismic) were combined into bi-axial loads following ASME B31.8 to assess driving margins.

From a sensitivity perspective, the wall thickness, SMYS, operating pressure and seismic load were the most significant determinants. Both under the ASCE 7 and the 2011 seismic event loading, it was shown either a positive or negative stress margin at the location was possible (see **Figure 12**). The resulting analysis revealed that, on average and under then-operating conditions, loads from the actual seismic event versus the ASCE 7 loads reduce the bi-axial margin by approximately 16%.

https://doi.org/10.52202/078572-0013

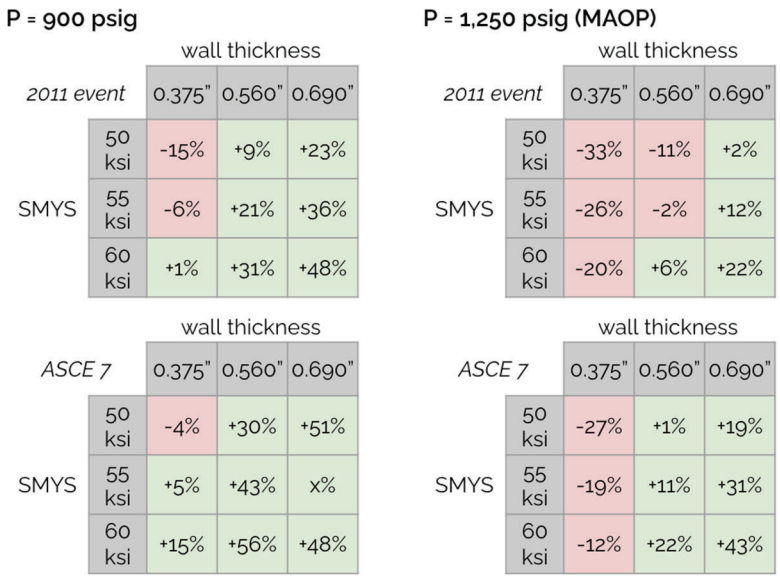

Figure 12. Parametric stress margin results for varying SMYS and wall thickness at the reported operating pressure (900 psig) and MAOP (1,250 psig) as well as the actual event and ASCE 7 seismic conditions

Under the reported operating conditions, and within reasonable ranges for wall thickness and SMYS, it was probable the pipe section at the location of the leak was operating with a negative stress margin during the seismic event in 2011. Stress concentrations which were likely present at the weld-end insulator were not included in the analysis and likely further eroded the stress margins.

Case Study 2: 2020, Denbury

Following an indication of a low-pressure alarm in February 2020, operators at Denbury closed and isolated a 9-mile segment of the 24" Delphi CO_2 pipeline at Mississippi Highway 433 crossing. Approximately 200 residents were evacuated and 45 were taken to the hospital. Following the all-clear from emergency response, an investigation began into the root-cause of the incident. Based on the metallurgical analysis and stress evaluations, it was concluded that soil movement (landslide) induced axial stresses sufficient to result in a rupture. The landslide was believed to have been promoted by usually high rainfall and not a singular rainfall event. In the area of the incident, there were no documented landslide events in the past, but the soil saturation trend was worsening in years prior (see **Figure 13**) – also, the seasonal January-March peaks were also becoming larger and larger.

https://doi.org/10.52202/078572-0013

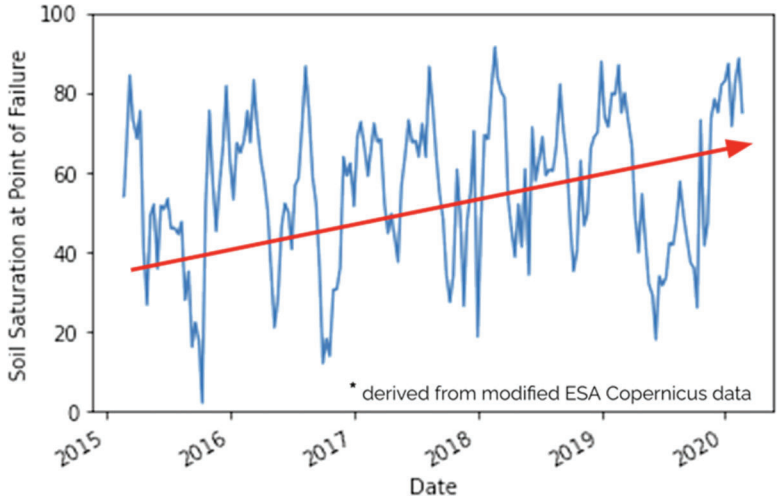

Figure 13. Historical soil saturation at the incident location leading up to the incident date

A static margin model of the slope (outlined previously) was developed for the area surrounding the incident location. SSURGO soil model data and USGS 3D Elevation Program (3DEP) LiDAR elevation models were used along with soil saturation data from remote sensing satellites. The results showed a downward trend in the slope margin (resisting-to-driving forces) year over year (see **Figure 14**).

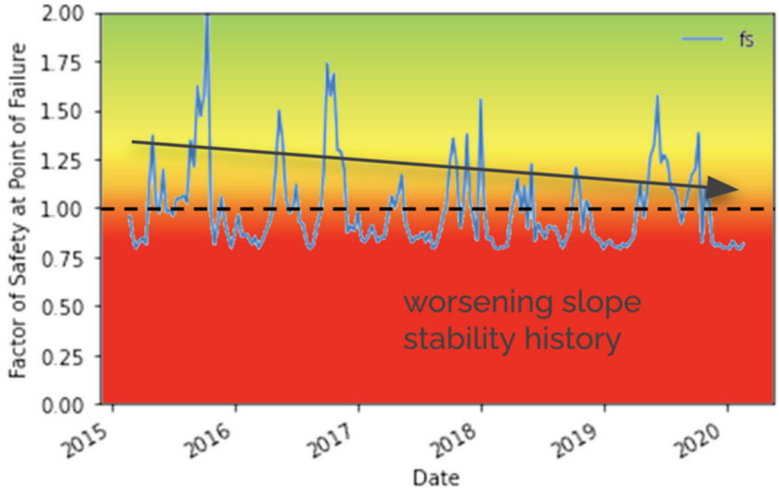

Figure 14. Historical slope static margin at the incident location leading up to the incident date

In the half decade leading up to the incident, the slope in question regularly went through periods of negative margin (highly susceptible to landslide). At the time of the incident, the entire slope face along the right-of-way adjacent to Highway 433 had a negative margin (see **Figure 15**).

https://doi.org/10.52202/078572-0013

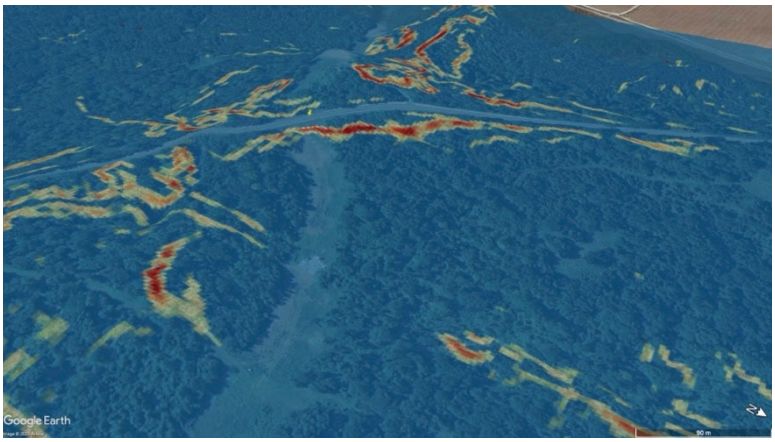

Figure 15. Static slope stability margin in area of Delphi pipeline and MS Highway 433 crossing (red indicates negative margin, yellow indicates no margin, etc.)

Because of the availability of both the PHMSA incident log data and the formal investigation report [32], sufficient details about the pipeline are known. The PHMSA incident log provided good detail of pipe parameters, so nominal pipe attributes and variations within specification were modeled. Given the age of the pipeline, the pipe surface conditions were varied between the installed condition (fusion bonded epoxy coating) and possible condition (bare).

The tool estimates other information about the pipeline required for loads development and margin assessment – for example the sections proximity to nearby road for live loading as well as soil properties required for evaluation of dead, live, and geohazard loads. To be as independent an evaluation as possible, SSURGO soil data and internal pipe-soil models were used instead of those in the investigation report (derived by testing of soils from the incident location).

Only a limited number of other model parameters were unknown – they were thus varied parametrically. For example, bedding design and surface finish (varied across all options), temperature conditions varied based on historical NOAA data, etc. The tool was then used to evaluate potential exposure to geohazards – for the affected section a seismic and landslide load case was found. The hoop (dead load, live load, and operating pressure) and longitudinal loads (operating pressure, thermal, seismic, and landslide) were combined into bi-axial loads following ASME B31.4 to assess driving margins.

Under the nominal conditions and pipe attributes and using average values for the soil friction and stiffnesses, the combined stress and margin at MAOP (2,160 psig) are almost nil. Namely, the hoop margin is +3% and the longitudinal margin is about 0%. At the operating pressure at the time of failure (1,336 psig) however, the hoop margin was +67% and the longitudinal margin +24%. However, at this location, the longitudinal margin is highly sensitive to the axial soil friction, which is sensitive to soil density and friction angle. For the soil type (clay) at the failure location, these properties can vary by as much as +/-30% (see **Figure 16)** - this in part increases the peak friction force at pipe-soil interface and subsequently increases the axial force on the affected pipe section exposed to the landslide.

https://doi.org/10.52202/078572-0013

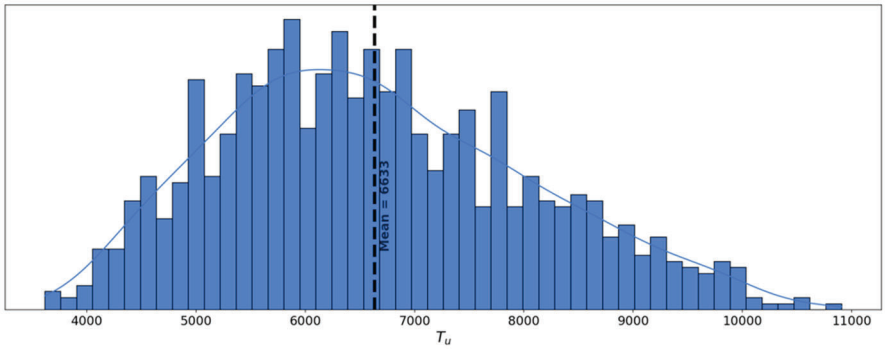

Figure 16. Histogram of peak friction force at pipe-soil interface for the affected section

When the soil properties are varied parametrically within these likely ranges, negative longitudinal stress margins are very possible (see **Figure 17**) – even at the lower operating pressure compared to MAOP.

T_u (lbf/in) \ MS_L	P_{OP} as % of MAOP			
	50%	61%	75%	100%
7k	+34%	+24%	+14%	-1%
8k	+25%	+16%	+7%	-6%
9k	+17%	+9%	0%	-10%
10k	+9%	0%	-4%	-15%

Figure 17. Parametric longitudinal stress margin results for varying peak friction force and operating pressure (as percent of MAOP)

Given the high susceptibility of the slope to landslide and under the reported operating conditions, it was probable the pipe section at the location of the incident was operating with nil or a negative stress margin during the landslide incident.

Case Study 3: 2021, Blue Racer Midstream

In February 2021, a Blue Racer Midstream 18" gathering line experienced a failure resulting in the unintentionally release of close to 22 million cubic feet of natural gas. The line was operating at a derated pressure (620 psig) compared to its MAOP (720 psig). A third-party SME determined the cause of the incident was earth movement, resulting in a circumferential crack in an area where stress corrosion cracking and general corrosion were found.

Using publicly available data from USGS [33], a differential LiDAR analysis between 2006 and 2020 was performed for the area around the affected pipe section. It revealed changes to the terrain around the incident location - especially near the hill toe and stream embankments (see **Figure 18**).

https://doi.org/10.52202/078572-0013

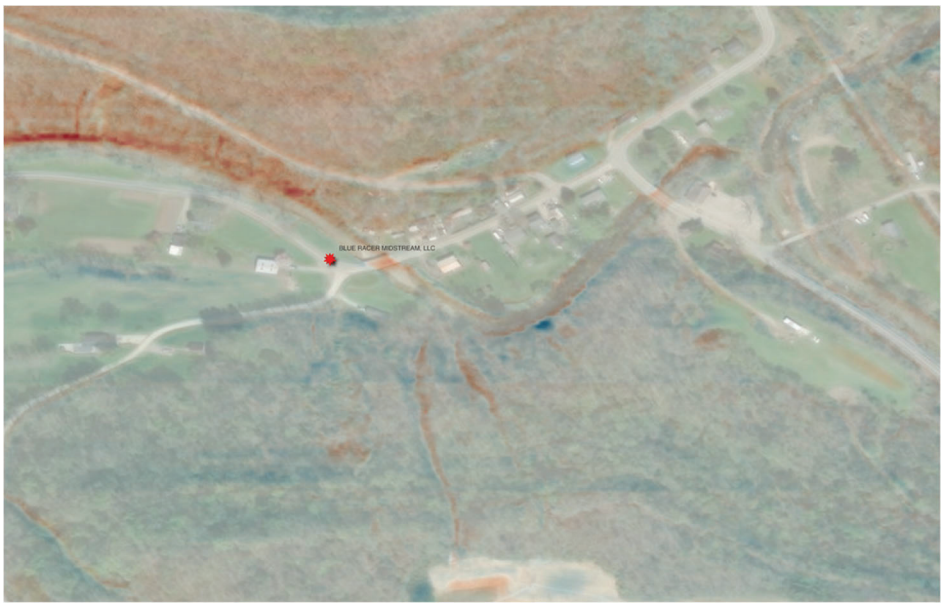

Figure 18. Change in elevation from differential LiDAR analysis using USGS 3DEP data

Therefore, some evidence exists supporting the conclusion that earth movement was the root-cause. A comparison between the observed displacements to the terrain and relatable model parameter ranges that equate to zero or negative margins in the affected section can be performed using the developed tool.

Information about the pipeline was relatively detailed in the PHMSA incident log. The affected section was API 5L steel pipe (electric resistance welded) with a 0.375" wall thickness and a SMYS of 42 ksi. The pipe surface treatment was coal tar, and the depth of cover was approximately 5 ft. However, information about the exact location and orientation of the pipe section is limited, and there is no apparent entry in National Pipeline Mapping System (NPMS) [34] or other public datasets. This makes it challenging to directly use the differential LiDAR analysis in the stress modeling. To overcome this, the nominal conditions were modeled and the earth movement loads varied to achieve a zero-margin state. A comparison to the differential LiDAR analysis can then be performed.

The tool estimates other information about the pipeline required for loads development and margin assessment – for example the sections proximity to nearby road for live loading as well as soil properties required for evaluation of dead, live, and geohazard loads. SSURGO soil data and internal pipe-soil models were used with reasonable variations in the soil stiffnesses and bearing capacities from soil properties.

Only a limited number of other model parameters were unknown – they were thus varied parametrically. For example, bedding design, pipe restraint and assembly design types, temperature conditions varied based on historical NOAA data, etc. The tool was then used to evaluate potential exposure to geohazards – for the affected section a seismic and earth movement load case were considered. The hoop (dead load, live load, and operating pressure) and longitudinal loads (operating pressure, thermal, seismic, and earth movement) were combined into bi-axial loads following ASME B31.8 to assess driving margins.

https://doi.org/10.52202/078572-0013

Under nominal conditions at the derated operating pressure with no earth movement load, the affected section had a hoop stress margin of approximately 41% and a longitudinal margin of over 200%. At MAOP, these margins decrease to approximately 20% and 180% respectively. Generally, pipe-soil interactions limit the pipe section displacement relative to any observed surface displacement. When accounting for the variation in soil conditions and the combined pipe-soil and pipe bending stiffness, this dampening can result in a reduction of 5-90% of the observed ground motion. At the derated operating pressure at the time of the incident, the earth movement change required to create zero stress margin is on average as follows: (i) lateral or vertical (uplift) ground curvature change ≥ 10^{-5} ft^{-1}; or (ii) vertical ground curvature (subsidence) change ≥ 10^{-4} ft^{-1}.

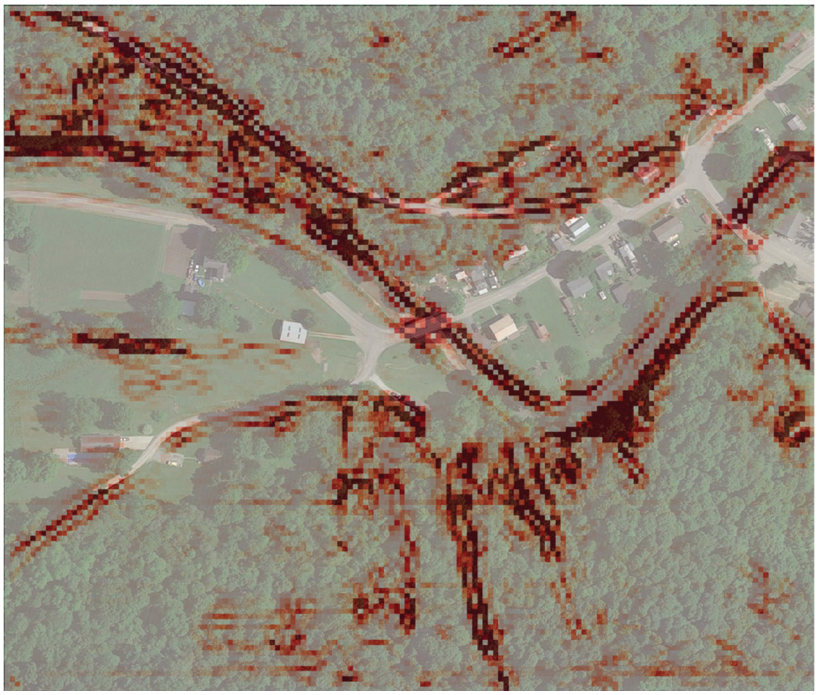

Figure 19. Terrain total curvature change between 2006 and 2020 in the area around the affected pipe section – dark red indicates areas where curvature ≥ 10^{-4} ft^{-1} zero-stress margin threshold

From the differential LiDAR analysis, the total curvature in the differenced elevation model is evaluated and compared to the zero-stress margin threshold of ≥ 10^{-4} ft^{-1} (see **Figure 19**). Several areas in the scene along slope toes and stream embankments have undergone change over the 14-year period and created topological curvature differences sufficient to drive stress margins in the affected pipe section to zero or negative regimes. If the affected pipe section crossed one or more of these areas, it would support the conclusion that bending loads caused from earth movement were the source of the circumferential cracking that led to the failure.

Discussion

While the case studies above are just a sample, they objectively make the case for the need to perform regular geohazard screening and monitoring. Given the cost of these incidents exceeded $8mm, there is a very compelling investment profile for a comprehensive geohazard program for any sized

https://doi.org/10.52202/078572-0013

operator. Beyond highlighting the utility of the developed tool, the case study analyses highlight several import takeaways.

Of upmost importance is the performance, fitness, and overall condition verification for older pipelines in operation today. While this will require investment from operators, there is a clear return on investment – especially given that loads from exposure to geohazards can compound over time and only act to increase the value proposition. Depending on the situation, differences between documented and actual conditions can have a material impact on stress margins under geohazard and non-geohazard loading. For example, differences between the recorded depth of cover (in the PHMSA record) and measurements observed as part of incident investigations are not uncommon – at locations of live loading, this can change pipe ovality and increase hoop stress.

Operators are required by PHMSA to perform baseline risk assessments are part of their integrity management program. This should include a comprehensive sensitivity analysis of both pipe, soil, and other relevant parameters. Soil and pipe characterization for every foot of the pipe network is obviously not practical, so accounting for possible variations with SME input is important. Furthermore, loading guidance from peer reviewed sources should be used at a minimum but analysis should also consider a survey for outlier events - even if they are greater than 6 σ environments.

Operators should continue to invest in their pipeline data model implementation, maintenance, and enhancement efforts. These models and their accuracies are a necessity for baseline analyses, proactive risk monitoring, and informed decision making. It is recommended that operators also consider adding variance and uncertainty details into these models as well. This would better inform end-users of these models of the level of fidelity they include.

Operators should have geohazard screening capability and monitoring programs in place separate from ground and aerial patrolling. While aerial and ground patrollers are a valuable resource in combatting pipeline risk, it is incredibly difficult for a human observer to detect onset of most geohazards. Screening and the use of a diversified set of geospatial measurement technologies can help better assess risks and inform decision making. For risks that are identified and needing to be monitored, it is imperative too that integrity engineers characterize the load ranges required to violate their organizations margin requirements and then work with vendors to pair these thresholds with the right sensing technologies. In some instances, these thresholds and measurement cadences may warrant LiDAR, but in other cases they may call for a more sensitive technology such as InSAR, global navigation satellite system interferometric reflectometry (GNSS-IR), or other solutions. Regardless, operators should regularly re-evaluate their risk and margins as conditions change – even if this is more frequent that what is required by PHMSA.

https://doi.org/10.52202/078572-0013

Acknowledgement

The authors gratefully thank the expertise and input of Jeff Suhey into the development and evaluation of the case studies. Furthermore, the authors thank Joseph Grenner for his help in researching the PHMSA advisories as well as all applicable CFR regulations.

Notice

This research was funded in part under the Department of Transportation, Pipeline and Hazardous Materials Safety Administration's Pipeline Safety Research and Development Program. The views and conclusions contained in this document are those of the authors and should not be interpreted as representing the official policies, either expressed or implied, of the Pipeline and Hazardous Materials Safety Administration, or the U.S. Government.

References

1. "Data and Statistics Overview | PHMSA." www.phmsa.dot.gov, www.phmsa.dot.gov/data-and-statistics/pipeline/data-and-statistics-overview.
2. "Potential for Damage to Pipeline Facilities Caused by Earth Movement and Other Geological Hazards | PHMSA." Dot.gov, 2019, www.phmsa.dot.gov/regulatory-compliance/phmsa-guidance/potential-damage-pipeline-facilities-caused-earth-movement-and. Accessed 9 Dec. 2024.
3. "Pipeline Safety: Potential for Damage to Pipeline Facilities Caused by Earth Movement and Other Geological Hazards | PHMSA." Dot.gov, 2022, www.phmsa.dot.gov/regulations/federal-register-documents/2022-11791. Accessed 9 Dec. 2024.
4. "Part 192 — Transportation of Natural and Other Gas by Pipeline: Minimum Federal Safety Standards." federalregister.gov, www.ecfr.gov/current/title-49/subtitle-B/chapter-I/subchapter-D/part-192.
5. "Part 195 — Transportation of Hazardous Liquids by Pipeline" federalregister.gov, www.ecfr.gov/current/title-49/subtitle-B/chapter-I/subchapter-D/part-195.
6. American Society of Mechanical Engineers (ASME). B31.4 - Pipeline Transportation Systems for Liquids and Slurries. 2022, www.asme.org/codes-standards/find-codes-standards/b31-4-pipeline-transportation-systems-liquids-slurries.
7. American Society of Mechanical Engineers (ASME). B31.8 - Gas Transmission and Distribution Piping Systems. 2022, www.asme.org/codes-standards/find-codes-standards/b31-8-gas-transmission-distribution-piping-systems
8. American Society of Civil Engineers (ASCE). Guideline for the Design of Buried Steel Pipe. 2001, www.americanlifelinesalliance.com/pdf/Update061305.pdf.
9. Esri. "Utility and Pipeline Data Model 2023 Is Released." Esri Community, 20 Nov. 2023, community.esri.com/t5/gas-and-pipeline-blog/utility-and-pipeline-data-model-2023-is-released/ba-p/1351728. Accessed 9 Dec. 2024.
10. Pipeline Open Data Standard (PODS) Association. "Home - PODS." PODS, 28 Oct. 2024, pods.org/. Accessed 9 Dec. 2024.

https://doi.org/10.52202/078572-0013

11. OpenStreetMap Foundation. “API - OpenStreetMap.” Wiki.openstreetmap.org, wiki.openstreetmap.org/wiki/API.
12. “Seismic Wave Propagation Analysis.” Passuite.com, passuite.com/kbase/doc/start/WebHelp_en/SeismicWave.htm. Accessed 23 May 2023.
13. United States Geological Survey (USGS). “API Documentation - Earthquake Catalog.” Earthquake.usgs.gov, earthquake.usgs.gov/fdsnws/event/1/.
14. American Society of Civil Engineers (ASCE). “ASCE7-16 Web Service Documentation.” usgs.gov, 2019, earthquake.usgs.gov/ws/designmaps/asce7-16.html. Accessed 9 Dec. 2024.
15. Worden, C. B., et al. “Probabilistic Relationships between Ground-Motion Parameters and Modified Mercalli Intensity in California.” Bulletin of the Seismological Society of America, vol. 102, no. 1, 1 Feb. 2012, pp. 204–221, https://doi.org/10.1785/0120110156. Accessed 24 Apr. 2021.
16. American Society of Civil Engineers (ASCE). Guideline for the Design of Buried Steel Pipe. 2001, www.americanlifelinesalliance.com/pdf/Update061305.pdf.
17. Mohraz, Bijan, and Fahim Sadek. Chapter 2 Earthquake Ground Motion and Response Spectra.
18. Donovan, N. C., “Earthquake Hazards for Buildings,” Building Practices for Disaster Mitigation, National Bureau of Standards, U.S. Department of Commerce, Building Research Services 46, 82-111, 1973.
19. Karamanos, Spyros A., et al. "Seismic Design of Buried Steel Water Pipelines." ASCE, 2014, Pg. 5
20. Karamanos, Spyros A., et al. "Seismic Design of Buried Steel Water Pipelines." ASCE, 2014, Pg. 5
21. Styron, Richard, and Marco Pagani. “The GEM Global Active Faults Database.” Earthquake Spectra, vol. 36, no. 1_suppl, 10 Aug. 2020, pp. 160–180, https://doi.org/10.1177/8755293020944182.
22. “Ghsc / National Seismic Hazard Model Project / Nshm-Fault-Sections · GitLab.” GitLab, code.usgs.gov/ghsc/nshmp/nshm-fault-sections. Accessed 2024.
23. Team, ASF APD/Tools. “Product Guide - HyP3.” Hyp3-Docs.asf.alaska.edu, hyp3-docs.asf.alaska.edu/guides/insar_product_guide/. Accessed 2024. Figure 1.
24. Mohseni, Omid. “Storm-Induced Slope Failure Susceptibility Mapping.“ Minnesota Department of Transportation, Jan. 2018, mdl.mndot.gov/_flysystem/fedora/2023-01/201805.pdf. Accessed 25 Jan. 2024.
25. Lockyear, Russell A. “Identification of Parameters for Predicting Long-Runout Landslides in the Western United States.” Repository.mines.edu, 2018, repository.mines.edu/handle/11124/172584. Accessed 25 Jan. 2024.
26. “National Geologic Map Database.” ngmdb.usgs.gov, ngmdb.usgs.gov/ngmdb/ngmdb_home.html. Accessed 2024.
27. “Subsidence Incident Reports | Florida Department of Environmental Protection.” floridadep.gov, 2010, floridadep.gov/fgs/sinkholes/content/subsidence-incident-reports. Accessed 2024.
28. Paine, Jeffrey, et al. Airborne and Ground Surveys of the April 2023 Daisetta Sinkhole, Liberty County, Texas Bureau of Economic Geology.
29. “Distribution, Transmission & Gathering, LNG, and Liquid Accident and Incident Data | PHMSA.” Dot.gov, 2019, www.phmsa.dot.gov/data-and-statistics/pipeline/distribution-transmission-gathering-lng-and-liquid-accident-and-incident-data.
30. “Summary of the 2011 M5.8 Mineral, Virginia Sequence.” Usgs.gov, 2024, earthquake.usgs.gov/earthquakes/eventpage/se609212/executive. Accessed 12 Dec. 2024.

31. "10-Year Anniversary of US's Most Widely Felt Earthquake | U.S. Geological Survey." Www.usgs.gov, www.usgs.gov/news/featured-story/10-year-anniversary-uss-most-widely-felt-earthquake.
32. "PHMSA Failure Investigation Report - Denbury Gulf Coast Pipelines, LLC | PHMSA." Dot.gov, 2022, www.phmsa.dot.gov/news/phmsa-failure-investigation-report-denbury-gulf-coast-pipelines-llc.
33. "3D Elevation Program | U.S. Geological Survey." Www.usgs.gov, www.usgs.gov/3d-elevation-program.
34. "National Pipeline Mapping System (NPMS)." Www.npms.phmsa.dot.gov, www.npms.phmsa.dot.gov/.

https://doi.org/10.52202/078572-0013